

## Innovative iteration technique for large deflection problem of annular plate

Y.Z. Chen\*

*Division of Engineering Mechanics, Jiangsu University, Zhenjiang, Jiangsu, 212013, P.R. China*

*(Received January 19, 2013, Revised March 29, 2013, Accepted May 24, 2013)*

**Abstract.** This paper provides an innovative iteration technique for the large deflection problem of annular plate. After some manipulation, the problem is reduced to a couple of ODEs (ordinary differential equation). Among them, one is derived from the plane stress problem for plate, and other is derived from the bending of plate. Since the large deflection for plate is assumed in the problem, the relevant non-linear terms appear in the resulting ODEs. The pseudo-linearization procedure is suggested to solve the problem and the nonlinear ODEs can be solved in the way for the solution of linear ODE. To obtain the final solution, it is necessary to use the iteration. Several numerical examples are provided. In the study, the assumed value for non-dimensional loading is larger than those in the available references.

**Keywords:** large deflection bending; pseudo-linearization of ODE; nonlinear analysis; iteration technique; annular plate

---

### 1. Introduction

In an earlier time, the governing equation for large deflection of a bending plate was proposed (Way 1934, Kármán 1940, Timoshenko and Woinowsky-Krieger 1959, Volmir 1963, Chia 1980, Cao 1996, 1997). Some researchers studied this problem by using analytical methods (Cao 1996, 1997). Using the variational theorem, the first order approximate solution for the large deflection problem of thin circular plate is obtained (He 2003).

A new theory for the non-axisymmetric elastic large deflection analysis of sector plates stiffened by a single eccentric rectangular cross-section radial stiffener was presented (Turvey and Salehi 1998). A solution was based on the use of fifth order polynomial radial basis function to build an approximation for the solution of two coupled nonlinear differential equations governing the finite deflection of thin plates (Naffa and Al-Gahtani 2007). An efficient meshless formulation was presented for large deflection of thin plates with immovable edges (Al-Gahtani and Naffa 2009). Based on the linear theory of thin plates, the incremental load technique was developed for solving the bending problem of a thin circular plate with large deflection (Lia *et al.* 2004). A semi-analytical approach was suggested for the geometrically nonlinear analysis of skew and trapezoidal plates subjected to out-of-plane loads (Shufrin *et al.* 2010). The method of linearization and construction of perturbation solutions for the Föppl von Kármán equations for the large

---

\*Corresponding author, Professor, E-mail: [chens@ujs.edu.cn](mailto:chens@ujs.edu.cn)

deflections of thin flat plates were discussed (Van Gorder 2012). A pseudo-linearization procedure of the nonlinear ordinary differential equation was suggested to solve the problem, where a simple iteration technique was used (Chen and Lee 2003).

Arefi and Rahimi (2012) studied the nonlinear analysis of functionally graded piezoelectric (FGP) annular plate with two smart layers as sensor and actuator. The normal pressure is applied on the plate. The geometric nonlinearity is considered in the strain-displacement equations based on Von-Kármán assumption.

This paper provides an innovative iteration technique for large deflection problem of annular plate. In the general formulation for the large deflection problem of plate, the total derivatives in the partial differential equation for deflection and the Airy stress function are equal to eight. In the present study for the annular plate, after some manipulation, the highest order derivative in the ODE for the deflection is equal to four and the derivatives for the radial stress is equal to two. Thus, the total derivatives in ODEs are equal to six. The boundary conditions at the starting point or the end point are equal to three. Therefore, the total boundary conditions are also equal to six. The pseudo-linearization procedure is suggested to solve the problem. In the procedure, for example, the non-linear term  $(dw/dx)^2$  is rewritten in the form  $(dw/dx)_{(j)}(dw/dx)$ , where  $(dw/dx)_{(j)}$  is a known function from the  $j$ -th iteration. Therefore, after using the pseudo-linearization procedure, the ODE becomes a linear one and the superposition method can be used. In order to obtain the final solution for the non-linear ODE, the iteration is necessary.

In the nonlinear problem, the final solution for the deflection depends on the non-dimensional loading “ $Q$ ”. In the innovative iteration technique, the initial iteration values of some functions for the loading  $Q_{i+1}$  are adopted from the previous solution for the loading  $Q_i$  ( $Q_i < Q_{i+1}$ ). This will significantly extend the range of solution for the non-dimensional loading. In the study, the value for non-dimensional loading is larger than those in the available references.

Finally, several numerical examples are provided which have not been obtained by other researchers.

## 2. Formulation of the governing equations and the boundary conditions

The governing equations and the boundary conditions for the large deflection problem of annular plate are introduced below. In the following analysis, we may repeat some previously obtained results (Way 1934, Kármán 1940, Timoshenko and Woinowsky-Krieger 1959, Volmir 1963, Chia 1980).

First, we consider the governing equation in the middle plane. In the middle plane, the geometry equation takes the form (Way 1934, Kármán 1940, Timoshenko and Woinowsky-Krieger 1959, Volmir 1963, Chia 1980).

$$\varepsilon_r = \frac{du}{dr} + \frac{1}{2} \left( \frac{dw}{dr} \right)^2, \quad \varepsilon_\phi = \frac{u}{r} \quad (1)$$

where  $u(r)$  represents radial displacement and  $w(r)$  is the deflection (Fig. 1),  $\varepsilon_r$  and  $\varepsilon_\phi$  represent two strain components.

From Eq. (1), the compatibility equation for displacement will be

$$\frac{d}{dr}(r\varepsilon_\phi) - \varepsilon_r = -\frac{1}{2} \left( \frac{dw}{dr} \right)^2 \quad (2)$$

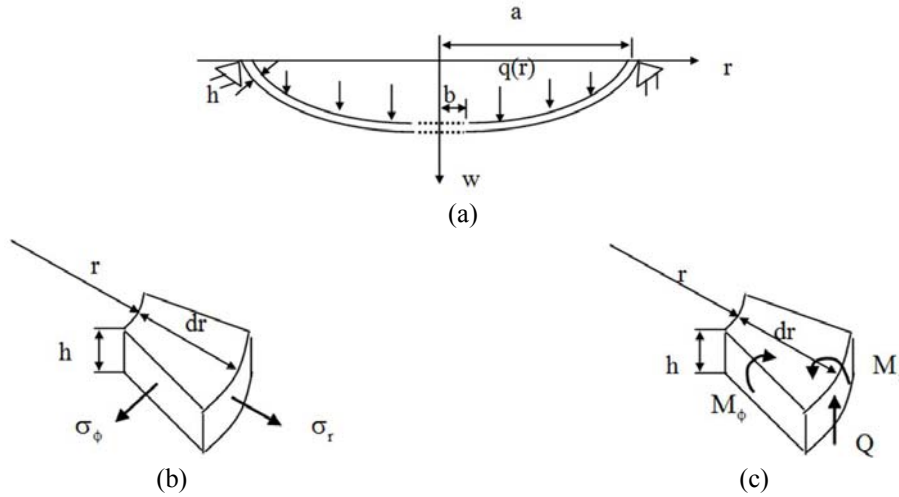


Fig. 1 (a) An annular plate with large deflection; (b) Stress components in the middle plane; and (c) Moment and shear force components in the bending problem

On the other hand, we have the following equilibrium equation (Fig. 1)

$$\frac{d}{dr}(r\sigma_r) - \sigma_\phi = 0 \quad \text{or} \quad \sigma_\phi = \frac{d}{dr}(r\sigma_r) \tag{3}$$

where  $\sigma_r$  and  $\sigma_\phi$  represent two stress components.

In addition, the constitute equation is as follows

$$\varepsilon_r = \frac{1}{E}(\sigma_r - \nu\sigma_\phi), \quad \varepsilon_\phi = \frac{1}{E}(\sigma_\phi - \nu\sigma_r) \tag{4}$$

where  $E$  is Young's modulus of elasticity, and  $\nu$  is the Poisson's ratio.

In Eq. (2), replacing  $\varepsilon_r$  and  $\varepsilon_\phi$  by  $\sigma_r$  and  $\sigma_\phi$  (using Eq. (4)), and using the equilibrium equation for  $\sigma_\phi$  and  $\sigma_r$  (using Eq. (3)) yields

$$\frac{1}{E} \left( \frac{d^2\sigma_r}{dr^2} + \frac{3}{r} \frac{d\sigma_r}{dr} \right) = -\frac{1}{2r^2} \left( \frac{dw}{dr} \right)^2 \tag{5}$$

Secondly, we consider the governing equation for bending (Fig. 1). The equilibrium condition for moment takes the form

$$\frac{dM_r}{dr} + \frac{M_r}{r} - \frac{M_\phi}{r} = -Q \tag{6}$$

where  $M_r$  and  $M_\phi$  are two moment components, and  $Q$  is the shear force component.

In addition, from the force equilibrium condition in z-direction, we have

$$Q = h\sigma_r \frac{dw}{dr} + \frac{q_1}{r} \quad \text{with} \quad q_1(r) = \int_b^r rq(r)dr + \text{constan}t \tag{7}$$

where “ $h$ ” is the thickness of plate, and  $q(r)$  is loading applied on the circular plate.

On the other hand, we have the constitute equation for the bending

$$M_r = -D\left(\frac{d^2w}{dr^2} + \frac{\nu}{r} \frac{dw}{dr}\right), \quad M_\phi = -D\left(\frac{1}{r} \frac{dw}{dr} + \nu \frac{d^2w}{dr^2}\right) \quad (8)$$

where

$$D = \frac{Eh^3}{12(1-\nu^2)} \quad (9)$$

Substituting Eqs. (7) and (8) into Eq. (6) yields

$$D\left(\frac{d^3w}{dr^3} + \frac{1}{r} \frac{d^2w}{dr^2} - \frac{1}{r^2} \frac{dw}{dr}\right) = \frac{q_1}{r} + h\sigma_r \frac{dw}{dr} \quad (10)$$

If we perform the following operator  $\frac{1}{r} \frac{d}{dr} \{r(\dots)\}$  to the both sides of Eq. (10), we have

$$D\left(\frac{d^4w}{dr^4} + \frac{2}{r} \frac{d^3w}{dr^3} - \frac{1}{r^2} \frac{d^2w}{dr^2} + \frac{1}{r^3} \frac{dw}{dr}\right) = q + h\left(\frac{\sigma_r}{r} \frac{dw}{dr} + \frac{d\sigma_r}{dr} \frac{dw}{dr} + \sigma_r \frac{d^2w}{dr^2}\right) \quad (11)$$

In the present study, a constant loading is applied along the plate face, or  $q(r) = q_o$ . Thus, Eq. (11) can be rewritten as

$$D\left(\frac{d^4w}{dr^4} + \frac{2}{r} \frac{d^3w}{dr^3} - \frac{1}{r^2} \frac{d^2w}{dr^2} + \frac{1}{r^3} \frac{dw}{dr}\right) = q_o + h\left(\frac{\sigma_r}{r} \frac{dw}{dr} + \frac{d\sigma_r}{dr} \frac{dw}{dr} + \sigma_r \frac{d^2w}{dr^2}\right) \quad (12)$$

For convenience in derivation, the subscript “ $r=c$ ”, for example in  $w|_{r=c}$  represents the deflection “ $w$ ” at the place  $r=c$ . For the bending problem, we can propose the following three types of boundary condition, from condition (b1), (b2) to (b3).

(b1) The clamped edge condition is as follows

$$w|_{r=c} = 0 \quad (13a)$$

$$\left.\frac{dw}{dr}\right|_{r=c} = 0 \quad (13b)$$

(b2) From Eq. (8), the simply-supported edge condition is as follows

$$w|_{r=c} = 0 \quad (14a)$$

$$M_r(r)|_{r=c} = 0 \quad (\text{or} \quad \left.\frac{d^2w}{dr^2} + \frac{\nu}{r} \frac{dw}{dr}\right|_{r=c} = 0) \quad (14b)$$

(b3) From Eqs. (6) and (8), the traction free edge condition is as follows

$$M_r(r)|_{r=c} = 0 \quad (\text{or} \quad \text{or} \quad \frac{d^2w}{dr^2} + \frac{\nu}{r} \frac{dw}{dr} \Big|_{r=c} = 0) \tag{15a}$$

$$Q(r)|_{r=c} = 0 \quad (\text{or} \quad \frac{d^3w}{dr^3} + \frac{1}{r} \frac{d^2w}{dr^2} - \frac{1}{r^2} \frac{dw}{dr} \Big|_{r=c} = 0) \tag{15b}$$

In the following analysis, the large deflection problem for an annular plate is considered (Fig. 2). In this case, the notation  $r=c$  may be understood as  $r=b$  (at the inner boundary of annular plate), or  $r=a$  (at the exterior boundary of annular plate).

For the plane stress problem in the middle plane, we can propose the following two types of boundary condition, from the condition (m1) to (m2).

(m1) The movable edge condition is as follows

$$\sigma_r|_{r=c} = 0 \tag{16}$$

(m2) From Eqs. (1), (3) and (4), the immovable edge condition is as follows

$$u|_{r=c} = r\varepsilon_\phi|_{r=c} = 0 \quad (\text{or} \quad \left( \sigma_r + \frac{r}{1-\nu} \frac{d\sigma_r}{dr} \right) \Big|_{r=c} = 0) \tag{17}$$

The real boundary conditions are composed of one of (b1), (b2), (b3) and one of (m1), (m2), for example, (b1) and (m2). Therefore, the boundary conditions for one edge, for example at  $r=b$ , is three. The total boundary conditions for two edges at  $r=b$  and  $r=a$ , are equal to six (= 2\*3). On the other hand, from the Eqs. (5) and (12), we see that, the total order of derivatives for  $d^j\sigma_r / dr^j$  and  $d^k w / dr^k$  is also equal to six.

Finally, we can make the following substitutions

$$r = as, \quad w = hW(s), \quad \sigma_r = \frac{Eh^2}{a^2} T(s), \quad q_o = \frac{Eh^4}{a^4} P_o \tag{18}$$

From Eq. (18) we see that,  $s$ ,  $W(s)$ ,  $T(s)$  and  $P_o$  represent some non-dimensional value.

After using those substitutions, from Eq. (5) and (12), we have

$$\frac{d^4W}{ds^4} + \frac{2}{s} \frac{d^3W}{ds^3} - \frac{1}{s^2} \frac{d^2W}{ds^2} + \frac{1}{s^3} \frac{dW}{ds} - 12(1-\nu^2) \left( \frac{T}{s} \frac{dW}{ds} + \frac{dT}{ds} \frac{dW}{ds} + T \frac{d^2W}{ds^2} \right) = 12(1-\nu^2)P_o \tag{19}$$

$(\alpha \leq s \leq 1, \quad \alpha = b/a)$

$$\frac{d^2T}{ds^2} + \frac{3}{s} \frac{T}{ds} + \frac{1}{2s^2} \left( \frac{dW}{ds} \right)^2 = 0 \quad (\alpha \leq s \leq 1, \quad \alpha = b/a) \tag{20}$$

### 3. Innovative iteration technique for solving non-linear ordinary differential equations

For some particular boundary conditions, a detailed description based on an innovative iteration technique for large deflection problem of annular plate is introduced below (Fig. 2).

In the formulation, at edge  $r=b$  (or  $s=\alpha=b/a$ ), the edge is assumed in the clamped condition for bending and immovable for plane stress. From Eqs. (13a, b) and (17), we have the following boundary conditions

$$W|_{s=\alpha} = 0, \quad \left. \frac{dW}{ds} \right|_{s=\alpha} = 0, \quad \left( T + \frac{\alpha}{1-\nu} \frac{dT}{ds} \right) \Big|_{s=\alpha} = 0 \quad (\alpha = b/a) \quad (21a, b, c)$$

In addition, at edge  $r=a$  (or  $s=1$ ), the edge is assumed in the simply supported condition for bending and movable for plane stress. From Eqs. (14a, b) and (16), we have

$$W|_{s=1} = 0, \quad \left( \frac{d^2W}{ds^2} + \nu \frac{dW}{ds} \right) \Big|_{s=1} = 0, \quad T|_{s=1} = 0 \quad (22a, b, c)$$

Some types of pseudo-linearization for the solution of nonlinear ODE were suggested previously (Chen and Lee 2003). One type of them is introduced below. In the formulation, it is assumed that the solution for functions  $W(s)$  and  $T(s)$  after  $j$ -th iteration is denoted by  $W_{(j)}(s)$  and  $T_{(j)}(s)$ . In addition, the ODEs shown by Eqs. (19) and (20) can be rewritten as

$$\begin{aligned} & \frac{d^4W}{ds^4} + \frac{2}{s} \frac{d^3W}{ds^3} - \frac{1}{s^2} \frac{d^2W}{ds^2} + \frac{1}{s^3} \frac{dW}{ds} \\ & - 12(1-\nu^2) \left( \frac{T_{(j)}}{s} \frac{dW}{ds} + \frac{dT_{(j)}}{ds} \frac{dW}{ds} + T_{(j)} \frac{d^2W}{ds^2} \right) = 12(1-\nu^2)P_o \end{aligned} \quad (23)$$

$(\alpha \leq s \leq 1, \quad \alpha = b/a)$

$$\frac{d^2T}{ds^2} + \frac{3}{s} \frac{T}{ds} + \frac{1}{2s^2} \frac{dW_{(j)}}{ds} \frac{dW}{ds} = 0 \quad (\alpha \leq s \leq 1, \quad \alpha = b/a) \quad (24)$$

Since the functions  $T_{(j)}(s)$ ,  $dT_{(j)}/ds$  and  $dW_{(j)}/ds$  are known beforehand, the ODEs shown by Eqs. (23) and (24) belong to the linear one.

For solving the ODEs shown by Eqs. (23) and (24) under conditions (21a,b,c) and (22a,b,c), the following technique is suggested.

First of all, we propose a particular solution for Eqs. (23) and (24) under the following conditions

$$W|_{s=\alpha} = 0, \quad \left. \frac{dW}{ds} \right|_{s=\alpha} = 0, \quad \left. \frac{d^2W}{ds^2} \right|_{s=\alpha} = 0, \quad \left. \frac{d^3W}{ds^3} \right|_{s=\alpha} = 0, \quad T|_{s=\alpha} = 0, \quad \left. \frac{dT}{ds} \right|_{s=\alpha} = 0 \quad (25)$$

The obtained solutions are denoted by  $W_p(s)$ ,  $T_p(s)$ .

Secondly, we propose three particular solutions for homogenous equations of Eqs. (23) and (24), or letting  $P_o = 0$  in right hand side of Eq. (23), under the following three sets of initial boundary conditions

$$W|_{s=\alpha} = 0, \quad \left. \frac{dW}{ds} \right|_{s=\alpha} = 0, \quad \left. \frac{d^2W}{ds^2} \right|_{s=\alpha} = 1, \quad \left. \frac{d^3W}{ds^3} \right|_{s=\alpha} = 0, \quad T|_{s=\alpha} = 0, \quad \left. \frac{dT}{ds} \right|_{s=\alpha} = 0 \quad (26)$$

$$W|_{s=\alpha} = 0, \quad \frac{dW}{ds}\Big|_{s=\alpha} = 0, \quad \frac{d^2W}{ds^2}\Big|_{s=\alpha} = 0, \quad \frac{d^3W}{ds^3}\Big|_{s=\alpha} = 1, \quad T|_{s=\alpha} = 0, \quad \frac{dT}{ds}\Big|_{s=\alpha} = 0 \quad (27)$$

$$W|_{s=\alpha} = 0, \quad \frac{dW}{ds}\Big|_{s=\alpha} = 0, \quad \frac{d^2W}{ds^2}\Big|_{s=\alpha} = 0, \quad \frac{d^3W}{ds^3}\Big|_{s=\alpha} = 0, \quad T|_{s=\alpha} = 1, \quad \frac{dT}{ds}\Big|_{s=\alpha} = -\frac{1-\nu}{\alpha} \quad (28)$$

The relevant solutions under the conditions Eqs. (26), (27) and (28) are denoted by  $W_1(s)$ ,  $T_1(s)$ ,  $W_2(s)$ ,  $T_2(s)$  and  $W_3(s)$ ,  $T_3(s)$ , respectively.

Thus, the investigated solutions can be assumed in the forms

$$\begin{aligned} W(s) &= W_p(s) + c_1W_1(s) + c_2W_2(s) + c_3W_3(s) \\ T(s) &= T_p(s) + c_1T_1(s) + c_2T_2(s) + c_3T_3(s) \end{aligned} \quad (29)$$

Furthermore, the three undetermined coefficients  $c_1$ ,  $c_2$  and  $c_3$  can be determined by the conditions Eqs. (22a, b, c).

Note that the initial boundary conditions Eqs. (21a, b, c) for the functions  $W(s)$  and  $T(s)$  are involved in the assumed boundary conditions shown by Eqs. (25) to (28). Thus, the solution satisfying the boundary conditions Eqs. (21a, b, c) and (22a, b, c) is obtainable, which is denoted by  $W_{(j+1)}(s)$  and  $T_{(j+1)}(s)$ .

The relevant initial boundary value problem can easily be solved numerically by using the Runge-Kutta method (Hildebrand 1974). Assume that the iteration is convergent. In this case, when the maximum deviation for the function  $W(s)$  and  $T(s)$  after  $N$ -th iteration satisfies the following conditions

$$\max|W_{(N)}(s) - W_{(N+1)}(s)| < \varepsilon_1, \quad \max|T_{(N)}(s) - T_{(N+1)}(s)| < \varepsilon_2 \quad (30)$$

The approximate solution is obtained. Otherwise, we make the next round iteration. In Eq. (30),  $\varepsilon_1$  and  $\varepsilon_2$  are two small values.

#### 4. Numerical examples

Numerical examples for large deflection of an annular plate are presented below (Fig. 2). In the examples,  $M=100$  divisions are used in the solution of the ODEs Eqs. (23) and (24). In addition,  $\varepsilon_1 = \varepsilon_2 = 10^{-6}$  is used for the error tolerance. Two examples are introduced below.

##### Example 4.1

In the first example, the boundary conditions were shown by Eqs. (21a, b, c) and (22a, b, c). At the edge  $r = b$  (or  $s = \alpha = b/a$ ), the edge is assumed in the clamped condition for bending and immovable for plane stress problem, and they are as follows (Fig. 2(a)).

$$W|_{s=\alpha} = 0, \quad \frac{dW}{ds}\Big|_{s=\alpha} = 0, \quad \left( T + \frac{\alpha}{1-\nu} \frac{dT}{ds} \right)\Big|_{s=\alpha} = 0 \quad (\alpha = b/a) \quad (21a, b, c)$$

In addition, at the edge  $r = a$  (or  $s = 1$ ), the edge is assumed in the simply supported condition for bending and movable for plane stress, and they are as follows (Fig. 2(a))

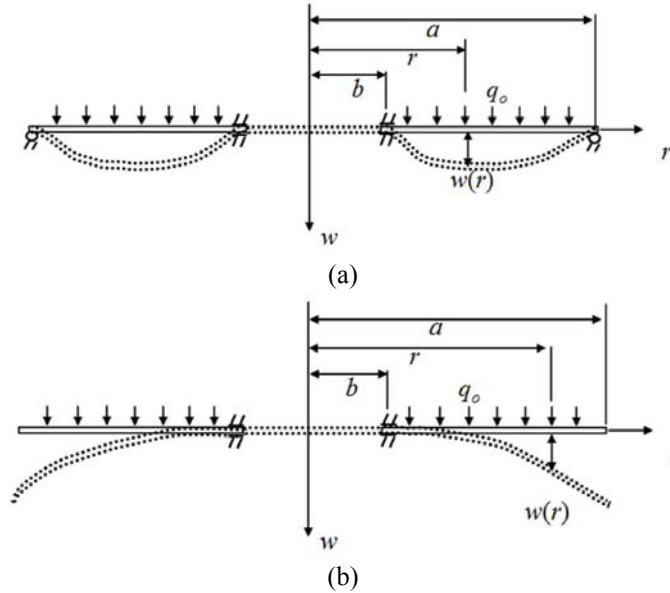


Fig. 2 Two boundary conditions: (a) at  $r = b$ , clamped condition for bending and immovable for plane stress, and at  $r = a$ , simply supported condition for bending and movable for plane stress, used for Example 4.1; (b) at  $r = b$ , clamped condition for bending and immovable for plane stress, and at  $r = a$ , traction free condition for bending and movable for plane stress, used for Example 4.2

$$W|_{s=1} = 0, \quad \left( \frac{d^2W}{ds^2} + \nu \frac{dW}{ds} \right) \Big|_{s=1} = 0, \quad T|_{s=1} = 0 \tag{22a, b, c}$$

For the cases (a)  $\alpha = 0.2$  and  $0.5$  ( $\alpha = b/a$ ), (b)  $P_o = 20, 40, 60, 80, 100$ , the calculated results for the non-dimensional deflection  $W(s)$  and the stress  $T(s)$  are expressed by

$$W(s) = f(\alpha, P_o, s) \tag{31}$$

$$T(s) = g(\alpha, P_o, s) \tag{32}$$

In the computation, an innovative iteration technique is used. In the technique, for example, in the case of  $P_o = 40$ , the first approximation solution for  $W(s)$  and  $T(s)$ , or the terms  $W_1(s)$  and  $T_1(s)$  for the first iteration in Eqs. (23) and (24) are adopted from the final relevant solution for the case of  $P_o = 20$ . A real computation proves that the iteration is convergent in general.

In the meantime, the results based on small deflection assumption are expressed as

$$W(s) = f_o(\alpha, P_o, s) \tag{33}$$

The computed results for  $f(\alpha, P_o, s)$ ,  $g(\alpha, P_o, s)$  and  $f_o(\alpha, P_o, s)$  are plotted in Figs. 3 to 6, respectively. Simply deleting some terms in Eq. (23), the deflection under small deflection or Kirchoff assumption is obtainable.

From plotted results we see that the ratio  $\alpha$  has a significant influence to the final results. For example, in the case of  $\alpha = 0.2$ ,  $P_o = 20$  and  $s = 0.6$ , we have  $f/f_o = 0.9416$ . That is to say the result based on the small deflection assumption provides an accurate result in this case. However, in the case of  $\alpha = 0.2$ ,  $P_o = 100$  and  $s = 0.6$ , we have  $f/f_o = 0.6125$ . That is to say the result based on the small deflection assumption has a larger deviation to the result based on the large deflection assumption in this case.

The computed results are quite different in the case  $\alpha = 0.5$ . For example, in the case of  $\alpha = 0.5$ ,  $P_o = 20$  and  $s = 0.75$ , we have  $f/f_o = 0.9987$ . In addition, in the case of  $\alpha = 0.5$ ,  $P_o = 100$  and  $s = 0.75$ , we have  $f/f_o = 0.9859$ . That is to say the result based on the small deflection assumption provides a sufficient accurate result in the case of  $\alpha = 0.5$ .

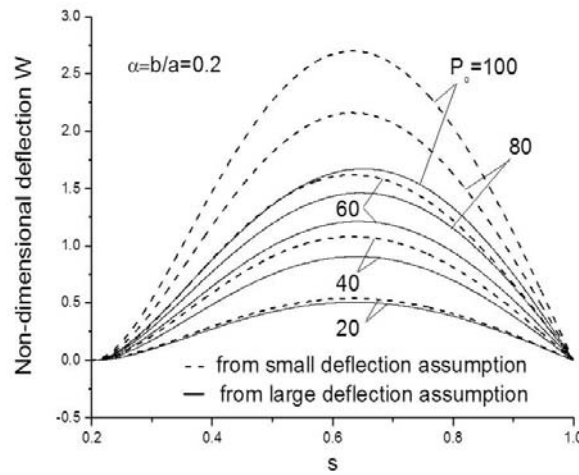


Fig. 3 Non-dimensional deflections  $W(s) = f(\alpha, P_o, s)$  (from large deflection assumption, with the solid curves) and  $W(s) = f_o(\alpha, P_o, s)$  (from small deflection assumption, with the dash curves), for  $\alpha = 0.2$  and  $P_o = 20, 40, 60, 80, 100$  (see Fig. 2(a) and Eqs. (31) and (33))

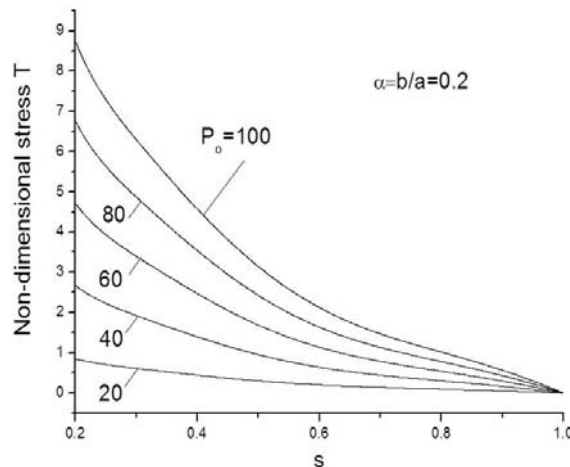


Fig. 4 Non-dimensional radial stress  $T(s) = g(\alpha, P_o, s)$  under large deflection assumption, for  $\alpha = 0.2$  and  $P_o = 20, 40, 60, 80, 100$  (see Fig. 2(a) and Eq. (32))

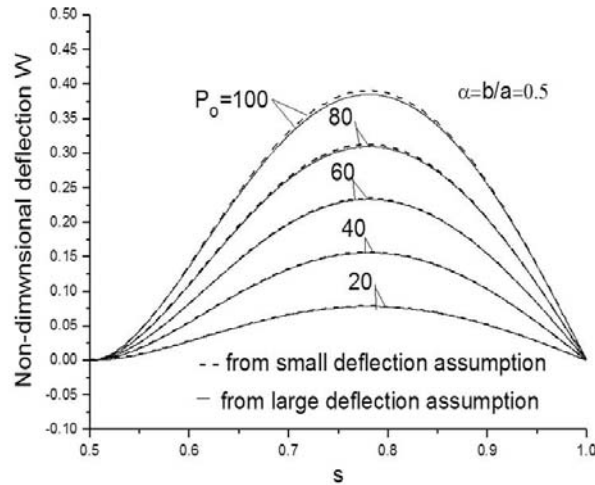


Fig. 5 Non-dimensional deflections  $W(s) = f(\alpha, P_o, s)$  (from large deflection assumption, with the solid curves) and  $W(s) = f_o(\alpha, P_o, s)$  (from small deflection assumption, with the dash curves), for  $\alpha = 0.5$  and  $P_o = 20, 40, 60, 80, 100$  (see Fig. 2(a) and Eqs. (31) and (33))

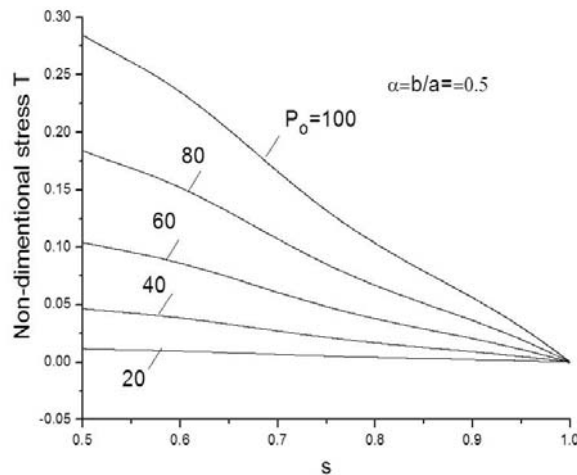


Fig. 6 Non-dimensional radial stress  $T(s) = g(\alpha, P_o, s)$  under large deflection assumption, for  $\alpha = 0.5$  and  $P_o = 20, 40, 60, 80, 100$  (see Fig. 2(a) and Eq. (32))

In addition, in the case of  $\alpha = 0.2$ ,  $P_o = 100$  and  $s = 0.2$ , we have  $T_{\max} = 8.7575$ . However, in the case of  $\alpha = 0.5$ ,  $P_o = 100$  and  $s = 0.5$ , we have  $T_{\max} = 0.2848$ . That is to say a large span of the annular plate will cause a significant radial stress  $T$ .

#### Example 4.2

In the second example, at edge  $r = b$  (or  $s = \alpha = b/a$ ), the edge is assumed in the clamped condition for bending and immovable for plane stress condition. From Eqs. (13a, b) and (17), we have the following boundary conditions (Fig. 2(b))

$$W|_{s=\alpha} = 0, \quad \frac{dW}{ds}\Big|_{s=\alpha} = 0, \quad \left( T + \frac{\alpha}{1-\nu} \frac{dT}{ds} \right)\Big|_{s=\alpha} = 0, \quad (\alpha = b/a) \quad (34a, b, c)$$

In addition, at the edge  $r = a$  (or  $s = 1$ ), the edge is assumed in the traction free condition for bending and movable for plane stress. From Eqs. (15a, b) and (16), we have (Fig. 2(b))

$$\left( \frac{d^2W}{ds^2} + \nu \frac{dW}{ds} \right)\Big|_{s=1} = 0, \quad \left( \frac{d^3W}{ds^3} + \frac{d^2W}{ds^2} - \frac{dW}{ds} \right)\Big|_{s=1} = 0, \quad T|_{s=1} = 0 \quad (35a, b, c)$$

The same technique mentioned in section 3 and Example 4.1 is used in the present example. Since the condition at the edge  $r = a$  (or  $s = 1$ ) is quite different to that in Example 4.1, the computed results must be different to those obtained in the Example 4.1.

For the cases (a)  $\alpha = 0.2$  and  $0.5$ , (b) two sets  $P_o = 1, 2, 3, 4, 5$ , and  $P_o = 20, 40, 60, 80, 100$ , the calculated results for the non-dimensional deflection  $W(s)$  and the stress  $T(s)$  are expressed by

$$W(s) = f(\alpha, P_o, s) \quad (31)$$

$$T(s) = g(\alpha, P_o, s) \quad (32)$$

In the computation, an innovative iteration technique is used.

In the meantime, the results based on small deflection assumption are expressed as

$$W(s) = f_o(\alpha, P_o, s) \quad (33)$$

For the cases (a)  $\alpha = 0.2$  and  $0.5$ , and  $P_o = 1, 2, 3, 4, 5$ , the computed results for  $f(\alpha, P_o, s)$ ,  $g(\alpha, P_o, s)$ , and  $f_o(\alpha, P_o, s)$ , are plotted in Figs. 7 to 10, respectively.

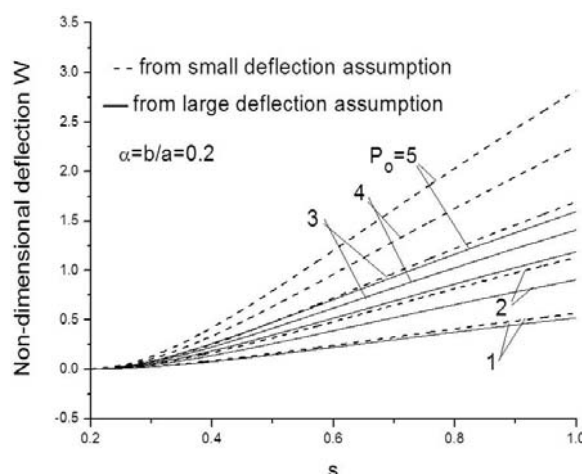


Fig. 7 Non-dimensional deflections  $W(s) = f(\alpha, P_o, s)$  (from large deflection assumption, with the solid curves) and  $W(s) = f_o(\alpha, P_o, s)$  (from small deflection assumption, with the dash curves), for  $\alpha = 0.2$  and  $P_o = 1, 2, 3, 4, 5$  (see Fig. 2 (b) and Eqs. (31) and (33))

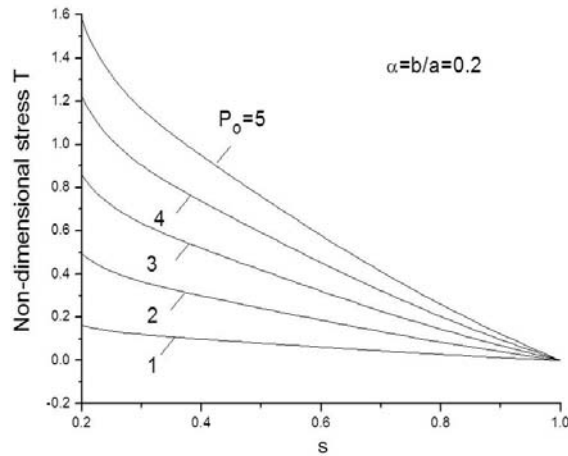


Fig. 8 Non-dimensional radial stress  $T(s) = g(\alpha, P_o, s)$  under large deflection assumption, for  $\alpha = 0.2$  and  $P_o = 1, 2, 3, 4, 5$  (see Fig. 2(b) and Eq. (32))

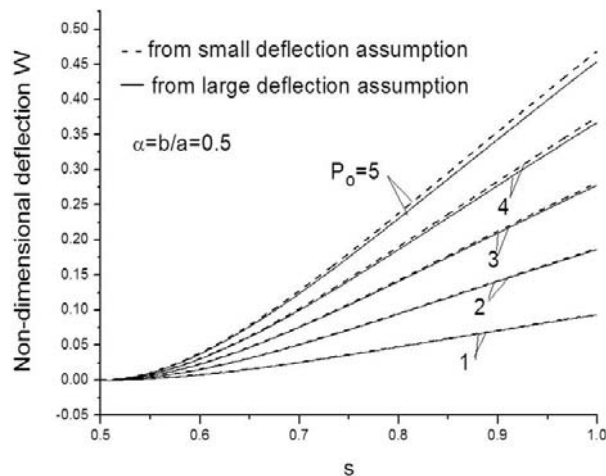


Fig. 9 Non-dimensional deflections  $W(s) = f(\alpha, P_o, s)$  (from large deflection assumption, with the solid curves) and  $W(s) = f(\alpha, P_o, s)$  (from small deflection assumption, with the dash curves), for  $\alpha = 0.5$  and  $P_o = 1, 2, 3, 4, 5$  (see Fig. 2(b) and Eqs. (31) and (33))

From plotted results we see that the ratio  $\alpha$  has a significant influence to the final results. For example, in the case of  $\alpha = 0.2$ ,  $P_o = 1$  and  $s = 1$ , we have  $f/f_o = 0.9245$ . That is to say the result based on the small deflection assumption provide an accurate result in this case. However, in the case of  $\alpha = 0.2$ ,  $P_o = 5$  and  $s = 1$ , we have  $f/f_o = 0.5655$ . That is to say the result based on the small deflection assumption has a larger deviation to the result based on the large deflection assumption in this case.

The computed results are quite different in the case  $\alpha = 0.5$ . For example, in the case of  $\alpha = 0.5$ ,  $P_o = 1$  and  $s = 1$ , we have  $f/f_o = 1$ . In addition, in the case of  $\alpha = 0.5$ ,  $P_o = 5$  and  $s = 1$ , we have  $f/f_o = 0.9695$ . That is to say the result based on the small deflection assumption provide a sufficient accurate result in the case of  $\alpha = 0.5$ .

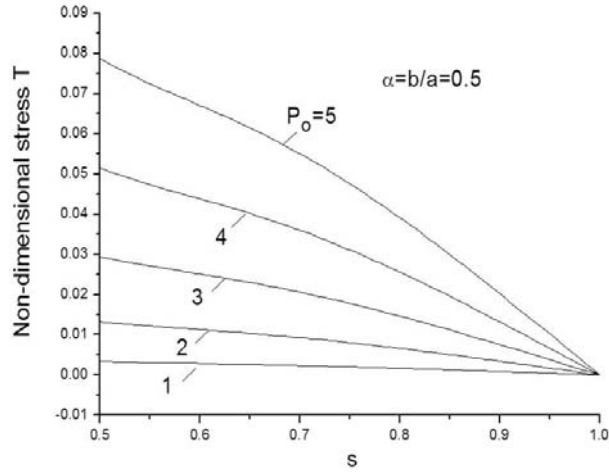


Fig. 10 Non-dimensional radial stress  $T(s) = g(\alpha, P_o, s)$  under large deflection assumption, for  $\alpha = 0.5$  and  $P_o = 1, 2, 3, 4, 5$  (see Fig. 2(b) and Eq. (32))

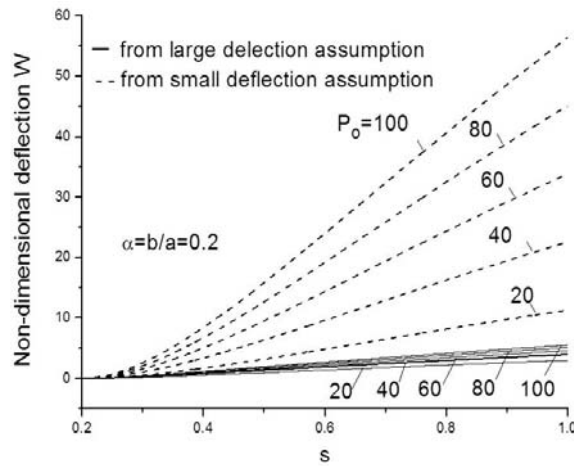


Fig. 11 Non-dimensional deflections  $W(s) = f(\alpha, P_o, s)$  (from large deflection assumption, with the solid curves) and  $W(s) = f(\alpha, P_o, s)$  (from small deflection assumption, with the dash curves),  $\alpha = 0.2$  and  $P_o = 20, 40, 60, 80, 100$  (see Fig. 2(b) and Eqs. (31) and (33))

In addition, in the case of  $\alpha = 0.2, P_o = 5$  and  $s = 0.2$ , we have  $T_{\max} = 1.5794$ . However, in the case of  $\alpha = 0.5, P_o = 5$  and  $s = 0.5$ , we have  $T_{\max} = 0.0787$ . That is to say a large span of the annular plate will cause a significant radial stress  $T$ .

For the cases (a)  $\alpha = 0.2$  and  $0.5$ , and  $P_o = 0, 40, 60, 80, 100$ , the computed results for  $f(\alpha, P_o, s)$ ,  $g(\alpha, P_o, s)$ , and  $f(\alpha, P_o, s)$ , are plotted in Figs. 11 to 14, respectively.

From plotted results we see that the ratio  $\alpha$  and the non-dimensional loading  $P_o$  have a significant influence to the final results. For example, in the case of  $\alpha = 0.2, P_o = 20$  and  $s = 1$ , we have  $f/f_o = 0.2670$ . In addition, in the case of  $\alpha = 0.2, P_o = 100$  and  $s = 1$ , we have  $f/f_o = 0.0982$ . That is to say the result based on the small deflection assumption has a larger deviation to the result based on the large deflection assumption in the case of  $P_o \geq 20$ .

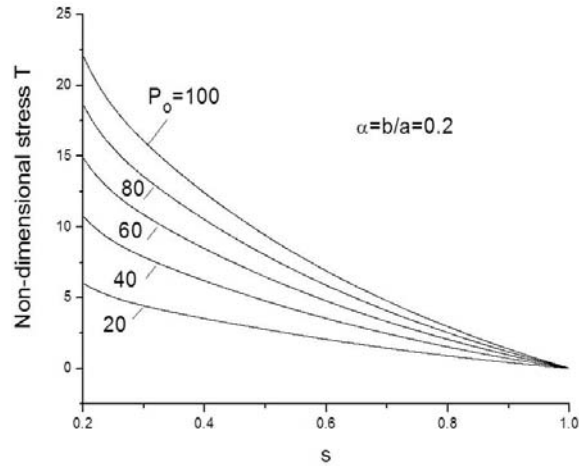


Fig. 12 Non-dimensional radial stress  $T(s) = g(\alpha, P_o, s)$  under large deflection assumption, for  $\alpha = 0.2$  and  $P_o = 20, 40, 60, 80, 100$  (see Fig. 2(b) and Eq. (32))

The computed results are quite different in the case  $\alpha = 0.5$ . For example, in the case of  $\alpha = 0.5$ ,  $P_o = 20$  and  $s = 1$ , we have  $f/f_o = 0.7614$ . In addition, in the case of  $\alpha = 0.5$ ,  $P_o = 100$  and  $s = 1$ , we have  $f/f_o = 0.3602$ . That is to say the small deflection assumption cannot provide accurate results in the case of  $P_o \geq 20$  and  $\alpha = 0.5$ .

In addition, in the case of  $\alpha = 0.2$ ,  $P_o = 100$  and  $s = 0.2$ , we have  $T_{\max} = 22.1322$ . However, in the case of  $\alpha = 0.5$ ,  $P_o = 100$  and  $s = 0.5$ , we have  $T_{\max} = 4.6249$ . That is to say a large span of the annular plate will cause a significant radial stress, or  $T$ .

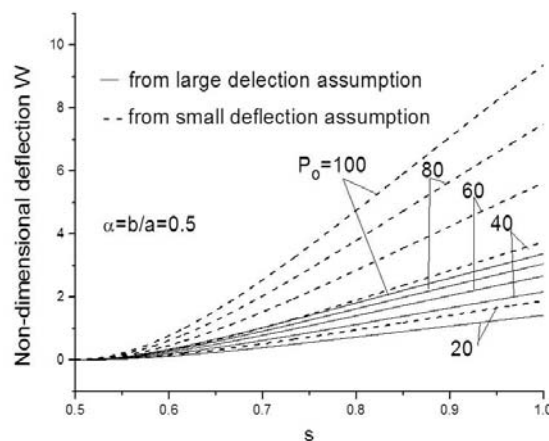


Fig. 13 Non-dimensional deflections  $W(s) = f(\alpha, P_o, s)$  (from large deflection assumption, with the solid curves) and  $W(s) = f(\alpha, P_o, s)$  (from small deflection assumption, with the dash curves), for  $\alpha = 0.5$  and  $P_o = 20, 40, 60, 80, 100$  (see Fig. 2(b) and Eqs. (31) and (33))

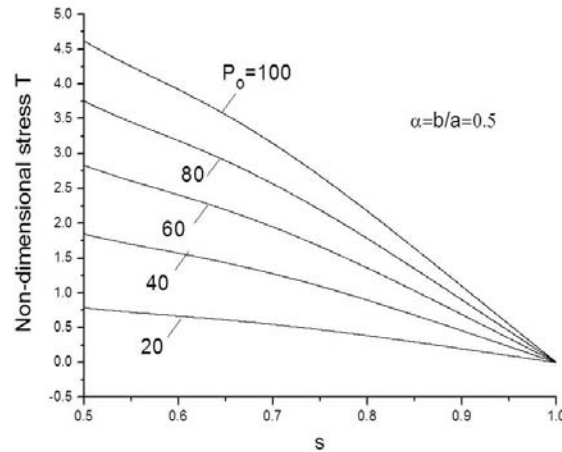


Fig. 14 Non-dimensional radial stress  $T(s) = g(\alpha, P_o, s)$  under large deflection assumption, for  $\alpha = 0.5$  and  $P_o = 20, 40, 60, 80, 100$  (see Fig. 2(b) and Eq. (32))

## 5. Conclusions

From above mentioned analysis, we see that the pseudo-linearization procedure in conjunction with the innovative iteration technique provides an effective way to solve the large deflection problem of a bending circular plate.

In the suggested method, the non-dimensional loading  $P_o$  is used for a rather high value. For example, we have used  $P_o = 100$  in the numerical example. However, in an earlier publication (Timoshenko and Woinowsky-Krieger 1959), only  $P_o = 12$  was used for a large deflection problem of plate.

It is seen from above-mentioned examples that the solution for the large deflection problem is rather complicated. The final solution may depend on the following factors: (a) the geometry of annular plate, (b) the applied non-dimensional loading  $P_o$  and (c) the boundary conditions. Clearly, if  $P_o \rightarrow 0$ , the solution from large deflection assumption will approach the solution based on the small deflection assumption. This result has been proved in the numerical example.

As claimed in the Example 4.2 (Fig. 2(b)), the ratio  $\alpha$  and the non-dimensional loading  $P_o$  have a significant influence to the final results. For example, in the case of  $\alpha = 0.2$ ,  $P_o = 20$  and  $s = 1$ , we have  $f/f_o = 0.2670$ . In addition, in the case of  $\alpha = 0.2$ ,  $P_o = 100$  and  $s = 1$ , we have  $f/f_o = 0.0982$ . That is to say the result based on the small deflection assumption has a larger deviation to the result based on the large deflection assumption in the case of  $P_o \geq 20$  in Example 4.2.

## References

- Al-Gahtani, H.J. and Naffa, M. (2009), "RBF meshless method for large deflection of thin plates with immovable edges", *Eng. Anal. Boun. Elem.*, **33**(2), 176-183.
- Arefi, M. and Rahimi, G.H. (2012), "Studying the nonlinear behavior of the functionally graded annular plates with piezoelectric layers as a sensor and actuator under normal pressure", *Smart Structures and Systems, Int. J.*, **9**(2), 127-143.
- Cao, J. (1996), "Computer extended perturbation solution of the large deflection of a circular plate. Part I

- Uniform loading with clamped edge”, *Quar. J. Mech. Appl. Math.*, **49**(2), 163-178.
- Cao, J. (1997), “Computer extended perturbation solution of the large deflection of a circular plate. Part II Control loading with clamped edge”, *Quar. J. Mech. Appl. Math.*, **50**(3), 333-347.
- Chen, Y.Z. and Lee, K.Y. (2003), “Pseudo-linearization procedure of nonlinear ordinary differential equations for large deflection problem of circular plates”, *Thin-walled Struct.*, **41**(4), 375-388.
- Chia, C.Y. (1980), *Nonlinear Analysis of Plates*, McGraw-Hill, New York.
- He, J. H. (2003), “A Lagrangian for von Kármán equations of large deflection problem of thin circular plate”, *App. Math. Comp.*, **143**(2-3), 543-549.
- Hildebrand, F.B. (1974), *Introduction to Numerical Analysis*, McGraw-Hill, New York.
- Kármán, T.H. (1940), “The engineering grapples with non-linear problems”, *Bull. Amer. Math. Soc.*, **46**, 615-683.
- Lia, Q.S., Liu, J. and Xiao, H.B. (2004), “A new approach for bending analysis of thin circular plates with large deflection”, *Int. J. Mech. Sci.*, **46**(2), 173-180.
- Naffa, M. and Al-Gahtani, H.J. (2007), “RBF-based meshless method for large deflection of thin plates”, *Eng. Anal. Boun. Elem.*, **31**(4), 311-317.
- Shufrin, I., Rabinovitch, O. and Eisenberger, M. (2010), “A semi-analytical approach for the geometrically nonlinear analysis of trapezoidal plates”, *Inter. J. of Mech. Sci.*, **52**(12), 1588-1596.
- Timoshenko, S.P. and Woinowsky-Krieger, S. (1959), *Theory of Plates and Shells*, McGraw-Hill, London.
- Turvey, G.J. and Salehi, M. (1998), “Large deflection analysis of eccentrically stiffened sector plates”, *Comput. Struct.*, **68**(1-3), 191-205.
- Van Gorder, R.A. (2012), “Analytical method for the construction of solutions to the Föppl von Kármán equations governing deflections of a thin flat plate”, *Inter. J. of Non-Linear Mech.*, **47**(3), 1-6.
- Volmir, A.C. (1963), *Large Deflection problem for Plates and Shells*, Science Press, Beijing. (Chinese translation from Russian)
- Way, S. (1934), “Bending of circular plate with large deflection”, *Trans. ASME*, **56**, 627-636.